PETROLEUM EXPLORATION AND DEVELOPMENT
Volume 46, Issue 5, October 2019
Online English edition of the Chinese language journal

Available online at www.sciencedirect.com
ScienceDirect

Cite this article as: PETROL. EXPLOR. DEVELOP., 2019, 46(5): 998–1005.

RESEARCH PAPER

Quantitative criteria for identifying main flow channels in complex porous media

LI Xizhe[1], LU Detang[2], LUO Ruilan[1], SUN Yuping[1,*], SHEN Weijun[3], HU Yong[1], LIU Xiaohua[1], QI Yadong[1], GUAN Chunxiao[1], GUO Hui[1]

1. PetroChina Research Institute of Petroleum Exploration & Development, Langfang 065007, China;
2. Department of Modern Mechanics, University of Science and Technology of China, Hefei 230026, China;
3. Institute of Mechanics, Chinese Academy of Sciences, Beijing 100190, China

Abstract: To identify the type of main flow channels of complex porous media in oil and gas reservoirs, the "main flow channel index" is defined as the ratio of comprehensive permeability obtained from well test to matrix permeability obtained from core analysis or well logging. Meanwhile, a mathematical model is established based on equivalent flow assumption, the classification method for main flow channels is put forward, and quantitative characterization of main flow channels is realized. The method has been verified by analysis of typical gas reservoirs. The study results show that the "main flow channel index" can quantitatively classify types of flow channels. If the index is less than 3, the matrix pore is the main flow channel; if the index is between 3 and 20, the fracture is the main flow channel and the matrix pore acts as the supplement one; if the index is more than 20, the fracture is the only seepage channel. The dynamic analysis of typical gas reservoirs shows that the "main flow channel index" can be used to identify the type of flow channel in complex porous media, guiding the classified development of gas reservoirs, and avoiding development risk.

Key words: porous media; matrix pore; fracture; flow channels; main flow channel index; quantitative identification criteria

Introduction

Porous media, composed of solid skeleton and pores, widely exist in engineering materials, organisms and formation media[1–2]. The rock of oil and gas reservoir is a typical porous medium, which generally contains pores, fractures, caverns and other forms of storage space and flow channels, and the forms of storage space and flow channels in different reservoirs are different. When oil and gas flow in the reservoir, they prefer to flow in the dominant paths with less resistance, and these dominant paths are the main flow channels[3–6]. In heterogeneous reservoirs, especially strongly heterogeneous reservoirs, the main flow channels generally appear in the form of faults and fractures, which with permeability several orders of magnitude higher than that of matrix pores, play an important role in controlling the accumulation and production of oil and gas. How to identify the types of main flow channels in oil and gas reservoirs quickly and accurately, and quantitatively characterize them, is directly related to the rationality and efficiency of the development policy of oil and gas fields.

Aiming at how to identify, describe and predict the main flow channels of porous media, scholars have carried out a lot of researches through laboratory experiments, theoretical analysis, numerical simulation and production performance analysis. Silliman et al.[7] described the forms of dominant flow pathways through laboratory experiments. Hestir et al.[8] and Datta-Gupta et al.[9] characterized the fluid flow in fractured rocks with classical hydrological inversion method. Ronayne et al.[10] and Kerrou et al.[11] estimated the hydrological parameters in the porous medium with the channel properties. Based on geophysical and hydrological data, Day-Lewis et al.[12] determined the dominant flow channels in the fractured rock. The above-mentioned studies are of great significance to deepen the understanding of main flow channels, but they are limited by laboratory experiments and numerical calculations, and haven't been verified by practical applications. Therefore, some researchers tried to identify the main flow channel with the permeability parameter closely related to the actual production. Warren et al.[13] and Guswa et al.[14] distinguished high and low permeability areas by using well test permeability. Amaefule et al.[15] and Al-Dhafeeri et al.[16] sorted out the hydraulic flow units and high permeability area in the reservoir through core experiments and production

Received date: 06 Apr. 2019; **Revised date:** 30 Jul. 2019.
*** Corresponding author.** E-mail: sunyuping01@petrochina.com.cn
https://doi.org/10.1016/S1876-3804(19)60256-9

data analysis. In complex reservoirs, the permeabilities obtained by well test and core analysis (or well logging) are not always consistent, and the main flow channels cannot be identified by a single parameter. Consequently, some researchers proposed other methods such as porosity-permeability modeling, flow zone index method and rock quality index method[17–21]. Unfortunately, these methods cannot evaluate the main flow channels in complex porous media accurately and quantitatively, and their conclusions are not universal to guide the identification of main flow channels.

In this work, in order to identify the types of main flow channels in oil and gas reservoirs, the main flow channel index was proposed, the quantitative relationship between large channel flow ratio and main flow channel index was established, the identification standard of main flow channels was set up, and the validity of this method was verified by the analysis of typical gas reservoirs.

1. Concept of main flow channel index and field laws

According to the different forms of porous media, the storage space and flow channels can be divided into matrix pores and fractures. Since the occurrence state of formation porous media is complex, it is difficult to describe all kinds of storage space and flow channels in realistic manner.

In order to tell the contributions of different channels to total flow capacity and identify the main flow channels, the following assumptions were made for the porous medium model: different flow channels had different seepage flow capacity, and the difference in seepage flow capacity between fracture system and matrix system is usually several orders of magnitude. Thus, according to the relative flow capacity of matrix pores and fractures, the flow channels were divided into two levels, and that is the benchmark channel represented by matrix pores and the large channel represented by fractures. The corresponding permeabilities are matrix permeability (K_m) and large channel permeability (K_f) respectively, and the comprehensive permeability (K_e) of the reservoir, that is the joint effect of the two.

In the oil and gas production, K_m can be obtained by core analysis or well logging and K_e can be obtained by well test. But it is difficult to get the permeability of large channels represented by fractures directly and quantitatively. Therefore, the main flow channel index which is defined as the ratio of reservoir comprehensive permeability to matrix permeability has been proposed and used to identify the types of main flow channel quantitatively.

$$\lambda = \frac{K_e}{K_m} \tag{1}$$

The procedure for determining the value of main flow channel index in gas field (reservoir) is as follows: (1) Taking a gas reservoir as an evaluation unit, some typical wells are selected, and the drainage area of these typical wells generally covers the whole reservoir. (2) Well test, well logging or core analysis are conducted on each typical gas well. (3) The comprehensive permeability is interpreted from well test data and the matrix permeability is the average value of all points in core analysis data or well logging data. (4) The main flow channel index of each typical well is calculated, which reflects the type of the flow channel in the drainage area of each well. (5) The average value of the main flow channel index of all typical gas wells represents the main flow channel characteristics of the whole gas reservoir.

Based on the above steps, the "main flow channel indexes" of 25 large gas fields in China were counted and analyzed, (Fig. 1). Combined with the reservoir characteristics and production performance of these gas fields, it is found that if the index is less than 3, the pore throat is the main flow channel, and the flow regime of gas wells is characterized by single porosity and single permeability system. If the index is between 3 and 20, the fracture is the main flow channel and the pore throat acts as the supplement one, and the reservoir exhibits the characteristics of dual porosity and dual permeability system. If the index is more than 20, the fracture can be considered as the only seepage channel, and the reservoir shows the characteristics of dual porosity and single permeability system.

2. Theoretical analysis of the boundary of main flow channel index

Based on the field laws shown from big data, the following theoretical model has been developed to determine the classification criterion of the main flow channel index.

2.1. Relationship between main flow channel index and large channel flow ratio

When a porous medium system includes fractures and matrix pores (Fig. 2), the following parameters can be used to indicate the relationship of pore, fracture and the whole system.

(1) Volume ratio of fracture system v_f: Represents the ratio of fracture system volume to the whole system volume.

(2) Volume ratio of matrix system v_m: Represents the ratio of the matrix system volume to the whole system volume.

The whole system volume equals to the sum of fracture

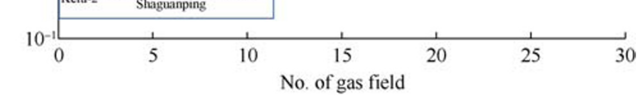

Fig. 1. Distribution of main flow channel index of 25 large gas fields in China.

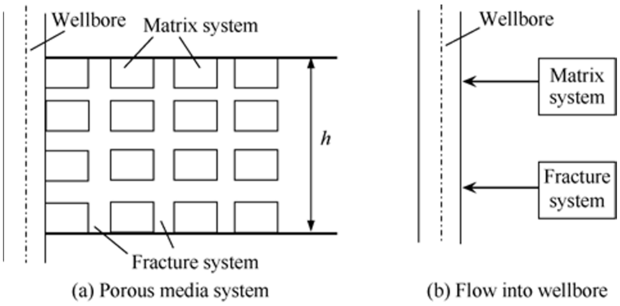

Fig. 2. Schematic diagram of porous media flow system.

system volume and matrix system volume:

$$v_{\mathrm{f}}+v_{\mathrm{m}}=1 \tag{2}$$

(3) Porosity of fracture system ϕ_{f}': Represents the proportion of fracture volume in the fracture system.

(4) Porosity of matrix system ϕ_{m}': Represents the proportion of pore volume in the matrix system.

(5) Porosity of fracture in the whole system ϕ_{f}: Represents the proportion of fracture volume in the whole system.

(6) Porosity of pore in the whole system ϕ_{m}: Represents the proportion of pore volume in the whole system.

According to the above definition, the following equations can be obtained:

$$\begin{cases}\phi_{\mathrm{f}}=v_{\mathrm{f}}\phi_{\mathrm{f}}' \\ \phi_{\mathrm{m}}=v_{\mathrm{m}}\phi_{\mathrm{m}}' \\ \phi=\phi_{\mathrm{f}}+\phi_{\mathrm{m}}=v_{\mathrm{f}}\phi_{\mathrm{f}}'+v_{\mathrm{m}}\phi_{\mathrm{m}}'\end{cases} \tag{3}$$

Select a cubic cell with matrix system and natural fracture system from the reservoir, with length L and cross-sectional area A. The matrix system has permeability of K_{m} and flow area of A_{m}; the fracture system has permeability of K_{f} and flow area of A_{f}. The flow area of the whole system $A=A_{\mathrm{m}}+A_{\mathrm{f}}$. Assume that the pressure at the two sides of the cell surface are p_1 and p_2 respectively, and the flow of fluid with viscosity of μ obey Darcy's law. Then, on the cell cross section, the flow rate of matrix system and fracture system can be expressed as

$$Q_{\mathrm{m}}=\frac{K_{\mathrm{m}}}{1.157\times10^{-2}\mu}A_{\mathrm{m}}\frac{p_1-p_2}{L} \tag{4}$$

$$Q_{\mathrm{f}}=\frac{K_{\mathrm{f}}}{1.157\times10^{-2}\mu}A_{\mathrm{f}}\frac{p_1-p_2}{L} \tag{5}$$

From equation (4) and equation (5), it can be obtained that the ratio of large channel flow to total flow is:

$$\eta=\frac{Q_{\mathrm{f}}}{Q_{\mathrm{f}}+Q_{\mathrm{m}}}=\frac{K_{\mathrm{f}}A_{\mathrm{f}}}{K_{\mathrm{f}}A_{\mathrm{f}}+K_{\mathrm{m}}A_{\mathrm{m}}} \tag{6}$$

It can be seen from equation (6) that the ratio of large channel flow to total flow is actually dependent on the product of permeability and flow area of fracture and matrix.

According to the definition of main flow channel index and Darcy's law, considering in general situation, $K_{\mathrm{m}}\ll K_{\mathrm{f}}$, $A_{\mathrm{m}}\gg A_{\mathrm{f}}$, then

$$\lambda=\frac{K_{\mathrm{e}}}{K_{\mathrm{m}}}=\frac{K_{\mathrm{f}}A_{\mathrm{f}}+K_{\mathrm{m}}A_{\mathrm{m}}}{K_{\mathrm{m}}\left(A_{\mathrm{f}}+A_{\mathrm{m}}\right)}\approx\frac{K_{\mathrm{f}}A_{\mathrm{f}}+K_{\mathrm{m}}A_{\mathrm{m}}}{K_{\mathrm{m}}A_{\mathrm{m}}}=1+\frac{K_{\mathrm{f}}A_{\mathrm{f}}}{K_{\mathrm{m}}A_{\mathrm{m}}}\approx1+\frac{K_{\mathrm{f}}}{K_{\mathrm{m}}}v_{\mathrm{f}} \tag{7}$$

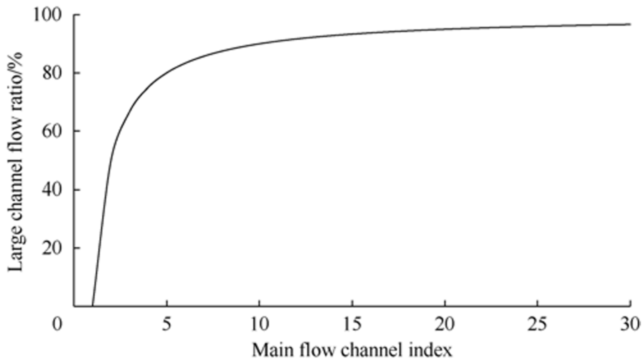

Fig. 3. Relationship between large channel flow ratio and main flow channel index.

By combining equation (6) and equation (7), the relationship between large channel flow ratio η and main flow channel index λ can be expressed as

$$\eta=\frac{K_{\mathrm{f}}A_{\mathrm{f}}}{K_{\mathrm{m}}A_{\mathrm{m}}+K_{\mathrm{f}}A_{\mathrm{f}}}=\frac{K_{\mathrm{f}}v_{\mathrm{f}}A}{K_{\mathrm{m}}A_{\mathrm{m}}+K_{\mathrm{f}}v_{\mathrm{f}}A}\approx\frac{K_{\mathrm{f}}v_{\mathrm{f}}}{K_{\mathrm{m}}+K_{\mathrm{f}}v_{\mathrm{f}}}=1-\frac{1}{\lambda} \tag{8}$$

According to equation (8), when the value of main flow channel index is relatively small, the contribution of large channel flow increases rapidly with the increase of main flow channel index, then the growth tends to be flat (Fig. 3). In order to obtain the maximum change point of the large channel flow ratio, the flow equivalent principle was used to transform the curve of Fig. 3 into the mathematical extremum problem.

2.2. Main flow channel index under the principle of flow equivalence

According to equation (6) and equation (8), and considering $K_{\mathrm{m}}\ll K_{\mathrm{f}}$, $A_{\mathrm{m}}\gg A_{\mathrm{f}}$, η can be expressed as

$$\eta=\frac{Q_{\mathrm{f}}}{Q_{\mathrm{f}}+Q_{\mathrm{m}}}\approx\frac{K_{\mathrm{f}}v_{\mathrm{f}}A}{K_{\mathrm{f}}v_{\mathrm{f}}A+K_{\mathrm{m}}A} \tag{9}$$

Equation (9) should have the equivalent form as shown in equation (10), with the same permeability but different cross-sectional area, by adjusting A_{f} and A_{m}, the same η value as that of equation (9) can be obtained.

$$\eta=\frac{Q_{\mathrm{f}}}{Q_{\mathrm{f}}+Q_{\mathrm{m}}}=\frac{Kv_{\mathrm{f}}A_{\mathrm{f}}}{Kv_{\mathrm{f}}A_{\mathrm{f}}+KA_{\mathrm{m}}} \tag{10}$$

In brief, given K_{f} and K_{m} under the condition of same cross-sectional area, η can be calculated, and the same η value can be obtained by changing A_{f} and A_{m} under the condition of same permeability, it is called flow equivalence principle. This principle aims to simplify the equation and solve it under the condition of equal flow.

According to the flow equivalence principle, referring to the well test analysis model and common pattern in the natural gas development, the circular area is adopted for research (Fig. 4). It is assumed that zone 1 in Fig. 4 represents the natural fracture system which contributes the flow rate of Q_{f}; Zone 2 represents the matrix pore system which contributes the flow rate of Q_{m}. By changing the areas of zone 1 and

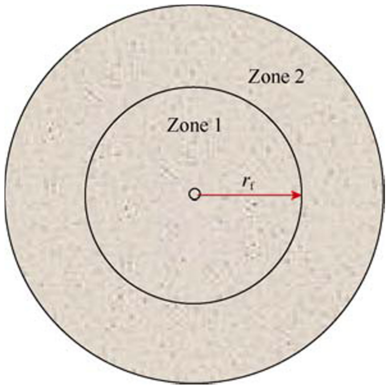

Fig. 4. Diagram of area change under the assumption of "same permeability".

zone 2, the large channel flow ratio η which is equivalent to the actual situation can be obtained.

When the gas well is produced at the flow rate Q, the total production is the sum of the production in zone 1 and zone 2. In a given production duration, there should be a gas drainage area which provides the dominant production. According to the assumption of “the same permeability” in the principle of flow equivalence, the production provided by this area can be equivalent to the production provided by the main flow channel.

2.2.1. Characteristic value of main flow channel

Based on the above ideas, assuming that at the instantaneous time of $t=\tau$, the fluid with mass of δ_m is injected in or produced from $M_0\left(x_0, y_0\right)$ point of porous medium, the equation and boundary conditions for fluid density ρ in infinite formation are as follows[22]:

$$\begin{cases} \dfrac{\partial^2 \rho}{\partial x^2}+\dfrac{\partial^2 \rho}{\partial y^2}=\dfrac{1}{3.6\chi}\dfrac{\partial \rho}{\partial t} \\ \rho\left(x \to \pm\infty, y \to \pm\infty, t\right)=\rho_i \\ \rho\left(x, y, t=\tau\right)=\begin{cases} \rho_i & \left(x, y\right) \notin M_0 \\ \infty & \left(x, y\right) \in M_0 \end{cases} \end{cases} \tag{11}$$

Through Fourier transform and inverse transform, the density distribution function of instantaneous source fluid is as follows:

$$\rho=\rho_i+\frac{\Gamma}{14.4\pi\chi\left(t-\tau\right)}\exp\left[-\frac{r^2}{14.4\chi\left(t-\tau\right)}\right] \tag{12}$$

where $r^2=\left(x-x_0\right)^2+\left(y-y_0\right)^2$, Γ is an undetermined constant, which is related to the mass of injection or production δ_m. $\Gamma=\dfrac{\delta_m}{h\phi}$ is obtained by integrating equation (12).

According to the equation of state of real gas, the relationship between density and pressure can be expressed as:

$$\rho=\frac{10^3 Mp}{RZT} \tag{13}$$

For a specific gas well, the formation temperature is constant, the gas composition is constant, and the average relative molecular weight of the gas is constant. Under the condition of constant temperature, the gas deviation factor is generally 0.9-1.1, that is, the density of gas is approximately linear with pressure. Meanwhile, the relationship of fluid volume and fluid mass is $\delta_m=\rho_i\delta_v$, and define $C_t=\dfrac{Z_i}{Zp_i}$, supposing $\tau=0$, then, the pressure distribution in the formation can be expressed as:

$$p\left(r, t\right)=p_i+\frac{\delta_v}{345.6\pi h\phi\chi C_t t}\exp\left(-\frac{r^2}{14.4\chi t}\right) \tag{14}$$

The maximum pressure differential is the key point. By deriving the equation (14) and taking the value of 0, it can be found that the time t^* at the maximum pressure differential has following relationship with the radius r^*,

$$r^{*\,2}=14.4\chi t^* \tag{15}$$

According to Darcy's law, the flow rate at any point r in the formation can be expressed as:

$$q\left(r, t\right)=\frac{Kh}{1.842\times10^{-3}\mu}r\frac{\partial p}{\partial r} \tag{16}$$

When a well in homogeneous formation produces at the flow rate of $\overline{q}$, the distribution of pressure differential $\Delta p\left(r, t\right)$ is as follows[22]:

$$\Delta p\left(r, t\right)=\frac{1.842\times10^{-3}\overline{q}B\mu}{2Kh}\left[-\mathrm{E_i}\left(\frac{r^2}{14.4\chi t}\right)\right] \tag{17}$$

The pressure gradient $\dfrac{\partial p}{\partial r}$ at any point r in the formation can be calculated by equation (17), and the flow rate at any point r can be obtained by substituting $\dfrac{\partial p}{\partial r}$ into equation (16):

$$q(r, t)=\overline{q}\exp\left(-\frac{r^2}{14.4\chi t}\right) \tag{18}$$

Equation (18) can be regarded as the contribution of flow within the region outside r, so the contribution of flow within the region inside r is as follows:

$$1-\frac{q(r, t)}{\overline{q}}=1-\exp\left(-\frac{r^2}{14.4\chi t}\right) \tag{19}$$

By substituting equation (15) into equation (19), we can get

$$1-\frac{q(r^*, t)}{\overline{q}}=1-\mathrm{e}^{-1}=0.632 \tag{20}$$

According to equation (20), 63.2% of the total flow is contributed by the region within radius r^*. That is to say, the ratio of the large channel flow corresponding to the point of the maximum pressure differential is 0.632. By substituting this value into equation (8), the main flow channel index λ is calculated of 2.7.

2.2.2. Identification criterion of main flow channel

For heterogeneous porous media, based on Fig. 3, we discuss the criterion for classifying the types of main flow channel.

(1) From the above analysis, it can be known that the “main flow channel index” of 2.7 is the dividing point from pore seepage to fracture seepage. In order to facilitate the field

application, this value can be taken as 3. It means if the index is less than 3, the matrix pore is the main flow channel, and otherwise, the fracture is the main flow channel.

(2) If the main flow channel index is more than 20, calculation by equation (8) shows that the proportion of large channel flow is more than 95%, and the benchmark channel flow is less than 5%. Based on the Ronald Aylmer Fisher Principle in statistics, at this time, benchmark channel flow is a small probability event, and the main channel flow occupies the absolute dominant position. So if the "main flow channel index" is more than 20, it can be considered that the fracture is the only flow channel.

3. Results and discussion

Taking three typical gas reservoirs as examples, the validity of "main flow channel index" boundary is further discussed from the point of view of field application.

3.1. Porous reservoir (Sebei gas field)

Sebei gas field[23] is located in Sanhu area of Qaidam Basin, with stable horizontal distribution and good lateral connectivity. The reservoir is dominated by primary pore, with only a small amount of secondary pore (Fig. 5). The reservoir has high porosity and permeability, with an average porosity of 30.95% and average permeability of 24.32×10^{-3} μm^2. The log-log curve of gas well pressure buildup test shows the percolation characteristics of homogeneous formation[24]. As shown in Fig. 6, the pressure derivative of gas well Se 2-23 enters radial flow stage after a short period of wellbore storage and transition flow.

Based on the core analysis data, well test data and logging data of 16 gas wells in different parts of Sebei gas field, the average "main flow channel index" of the gas field is 1.32, which means pore is the main flow channel.

This kind of gas reservoir has the characteristics of good physical properties and high productivity of gas wells. Although with edge/bottom water, water would advance evenly along the production zone, making the risk of water invasion low. Deploying gas wells in the structure high can prolong the period of water-free gas production and improve the ultimate recovery factor.

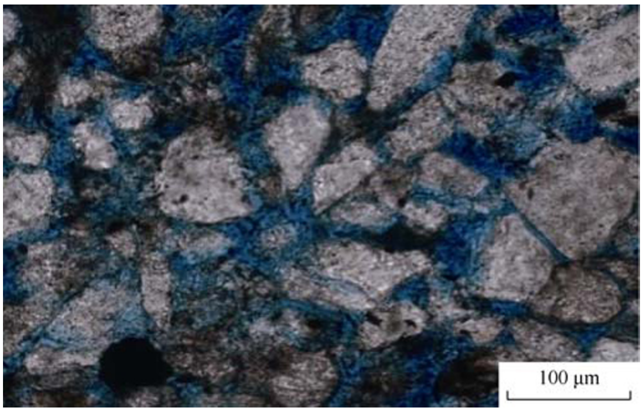

Fig. 5. Microscopic pore structure of core sample from Sebei gas field.

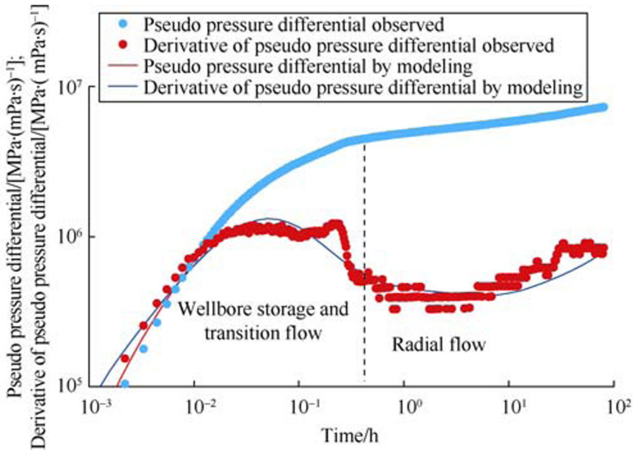

Fig. 6. Log-log fitting curve of gas well Se 2-23.

3.2. Fracture-pore type reservoir (Dina-2 gas field)

Dina-2 gas field[25] is located in Eastern Qiulitag structural belt of Kuqa Depression, Tarim Basin. It is a block gas reservoir with edge and bottom water in a nearly east-west anticline. The reservoir space includes primary intergranular pore, secondary intergranular pore and intragranular dissolved pore. Core analysis shows that its porosity is 4.90–8.97% and matrix permeability is $(0.09–1.11)\times10^{-3}$ μm^2. Core observation and imaging logging show that the reservoir has vertical and high-angle fractures with structural origin (Fig. 7). The fractures have an aperture of 0.05–0.15 mm and a density of 0.030–0.936/m, and are the main seepage channels of natural gas.

The log-log curve of gas well pressure buildup test shows the seepage characteristics of dual porosity and dual permeability system. As shown in log-log curve of Well DN22 (Fig. 8), after a short period of wellbore storage and transition flow, the logarithmic derivative curve shows a concave feature, the smaller the storage ratio, the deeper the concave curve is. The horizontal line represents the radial flow stage of the whole system.

Based on core analysis data, well test data and logging data of 22 gas wells in different parts of Dina gas field, the average "main flow channel index" of the gas field calculated is 10.32. That means the flow channel in this gas field is dominated by

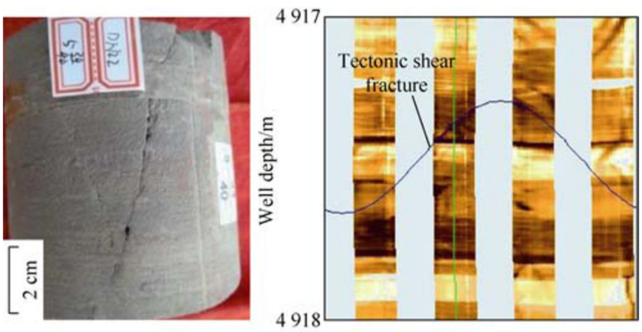

Fig. 7. Fracture distribution in core and imaging logging of Well DN22.

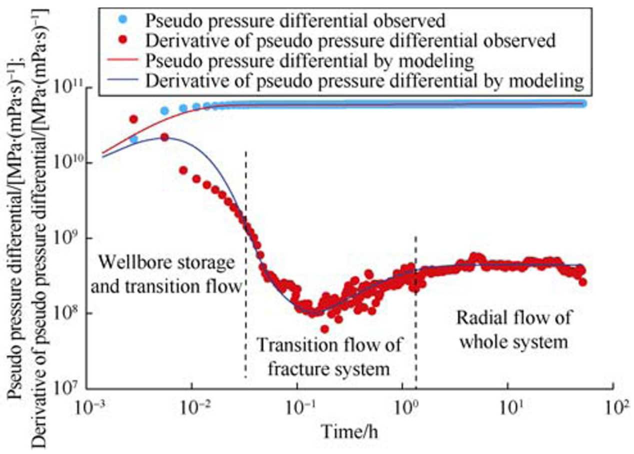

Fig. 8. Log-log fitting curve of Well DN22.

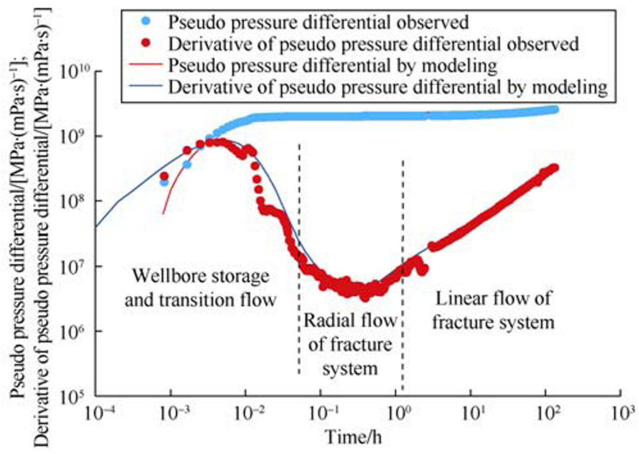

Fig. 10. Log-log fitting curve of Well Keshen 2-1-6.

fractures and supplemented by pores, which is consistent with the field production practice.

For this kind of gas reservoir, the matrix system can effectively supply gas to the fracture system. When the gas reservoir is developed in a balanced mode, the edge and bottom water would advance evenly, resulting in a longer period of water-free gas production.

3.3. Fractured reservoir (Keshen-2 gas field)

Keshen-2 gas field is located in the Kelasu structural belt of Kuqa Depression, Tarim Basin. It is an ultra-deep abnormally high pressure gas reservoir with edge and bottom water. It has multiple types of reservoir space, mainly intergranular pore, intragranular solution pore and micro-fracture (Fig. 9). Due to strong compaction, the reservoir has fine pore throats, low coordination number, a matrix porosity of 2%–6% and matrix permeability of $(0.01–0.1)\times10^{-3}$ μm^2.

Since the Himalayan Period, multi-stages of tectonic movements gave rise to a large number of structural fractures in Kuqa Depression, mainly high-angle fractures. Because of the tight matrix, fractures play a dominant role in natural gas production.

The log-log curve of gas pressure buildup test shows the percolation characteristics of dual porosity and single permeability system, with a long-term linear flow section, and the pseudo radial flow can't be seen during the later stage (Fig. 10).

Based on the core analysis data, well test data and logging data of 21 gas wells in different parts of Keshen-2 gas field, the average "main flow channel index" of the gas field calculated is 30.35, which indicates that the fracture can be regarded as the only flow channel. Three gas wells of Keshen2 gas field produced water after put into production for three months to four months, and the water production was 10–140 m^3/d. After 4 years of production, more than half of the gas wells produced water, which seriously impairs the productivity of gas wells and the production scale of the gas field[26].

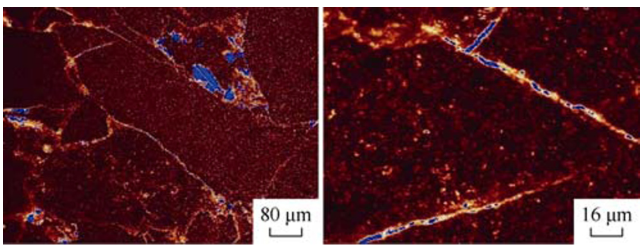

Fig. 9. Core samples from Keshen-2 gas field under laser confocal microscope.

For this kind of gas reservoirs with tight matrix and fractures, edge and bottom water is likely to channel along the fractures at high speed and cause water invasion, which makes the gas wells produce water early or even be flooded, and gas field development highly uncertain. Therefore, it is suggested that the gas field be developed in a balanced manner, and the matrix gas supply capacity and water invasion risk be fully taken into account to determine reasonable production of gas wells, and the wells be deployed at the structural highs far away from the gas-water contact[27–29].

4. Conclusions

The "main flow channel index" can be used to evaluate the main flow channels of porous media quantitatively. There is an obvious inflection point on the curve of relationship of "main flow channel index" and large channel flow ratio. With the increase of the "main flow channel index", the contribution of large channel flow increases rapidly in the initial stage, and the growth tends to be flat in the late stage.

If the index is less than 3, matrix pore is the main flow channel; if the index is between 3 and 20, the fracture is the main flow channel and the matrix pore acts as supplement; if the index is more than 20, the fracture is the only seepage channel.

Case study of typical gas reservoirs shows that the identification criterion of "main flow channel index" can effectively evaluate the main flow channel characteristics of underground complex porous media and provide technical support for the formulation of oil and gas field development policy.

Nomenclature

A—cross-sectional area of cubic cell, m^2;

A_f—cross-sectional area of fracture system, m^2;
A_m—cross-sectional area of matrix system, m^2;
B—volume coefficient, dimensionless;
C_t—comprehensive compressibility coefficient, MPa^{-1};
$\mathrm{E_i}$—exponential integral function;
h—reservoir thickness, m;
K_e—comprehensive permeability obtained by well test, μm^2;
K_m—matrix permeability obtained by core analysis or well logging, μm^2;
K_f—fracture permeability, μm^2;
K—flow equivalent formation permeability, μm^2;
L—length of cubic cell, m;
M—average mole mass of mixed gases, g/mol;
p_1, p_2—pressure at both ends of cubic cell, MPa;
p—reservoir pressure, MPa;
p_i—reservoir initial pressure, MPa;
Δp—pressure differential, MPa;
q—flow rate, m^3/d;
$\overline{q}$—well production, m^3/d;
Q_m—flow rate of matrix system, m^3/d;
Q_f—flow rate of fracture system, m^3/d;
r—drainage radius, m;
r^*—radius at the point of the maximum pressure differential, m;
r_f—equivalent drainage radius of fracture system, m;
R—universal gas constant, 8.314 J/(mol·K);
t—time, h;
t^*—time corresponding to the maximum pressure differential, h;
T—formation temperature, K;
v_f—volume ratio of fracture system, %;
v_m—volume ratio of matrix system, %;
x, y—abscissa and ordinate coordinates of any point in coordinate system, m;
x_0, y_0—abscissa and ordinate coordinates of fluid injection or production point, m;
Z—gas deviation factor, dimensionless;
Z_i—gas deviation factor under initial pressure, dimensionless;
Γ—undetermined constant, kg/m;
η—large channel flow ratio, f;
λ—main flow channel index, dimensionless;
μ—fluid viscosity, mPa·s;
ρ—fluid density of instantaneous source, kg/m^3;
ρ_i—initial fluid density, kg/m^3;
τ—initial time of instantaneous source injection or production, h;
ϕ—porosity of the whole system, %;
ϕ_f'—porosity of fracture system, %;
ϕ_m'—porosity of matrix system, %;
ϕ_f—porosity of fracture in the whole system, %;
ϕ_m—porosity of matrix in the whole system, %;
χ—pressure transmitting coefficient, 10^{-3} m^2/s;
δ_m—fluid mass, kg;
δ_V—fluid volume, m^3.

References

[1] LONG J C S, REMER J S, WILSON C R, et al. Porous media equivalents for networks of discontinuous fractures. Water Resources Research, 1982, 18(3): 645–658.

[2] BERKOWITZ B. Characterizing flow and transport in fractured geological media: A review. Advances in Water Resources, 2002, 25(8/9/10/11/12): 861–884.

[3] TSANG Y W, TSANG C F. Flow channeling in a single fracture as a two-dimensional strongly heterogeneous permeable medium. Water Resources Research, 1989, 25(9): 2076–2080.

[4] TSANG C F, NERETNIEKS I. Flow channeling in heterogeneous fractured rocks. Reviews of Geophysics, 1998, 36(2): 275–298.

[5] GOC R L, DREUZY J R D, DAVY P. An inverse problem methodology to identify flow channels in fractured media using synthetic steady-state head and geometrical data. Advances in Water Resources, 2010, 33(7): 782–800.

[6] NERETNIEKS I. Channeling effects in flow and transport in fractured rocks: Some recent observations and models. Stockholm: GEOVAL-87 International Symposium, 1987.

[7] SILLIMAN S E. An interpretation of the difference between aperture estimates derived from hydraulic and tracer tests in a single fracture. Water Resources Research, 1989, 25(10): 2275–2283.

[8] HESTIR K, MARTEL S J, VAIL S, et al. Inverse hydrologic modeling using stochastic growth algorithms. Water Resources Research, 1998, 34(12): 3335–3347.

[9] DATTA-GUPTA A, VASCO D W, LONG J C S, et al. Detailed characterization of a fractured limestone formation by use of stochastic inverse approaches. SPE Formation Evaluation, 1995, 10(3): 133–140.

[10] RONAYNE M J, GORELICK S M, CAERS J. Identifying discrete geologic structures that produce anomalous hydraulic response: An inverse modeling approach. Water Resources Research, 2008, 44(8): 1–16.

[11] KERROU J, RENARD P, FRANSSEN H J H, et al. Issues in characterizing heterogeneity and connectivity in non-multi Gaussian media. Advances in Water Resources, 2008, 31(1): 147–159.

[12] DAY-LEWIS F D, LANE J W, HARRIS J M, et al. Time-lapse imaging of saline-tracer transport in fractured rock using difference-attenuation radar tomography. Water Resources Research, 2003, 39(10): 1290.

[13] WARREN J E, PRICE H S. Flow in heterogeneous porous media. SPE Journal, 1961, 1(3): 153–169.

[14] GUSWA A J, FREYBERG D L. On using the equivalent conductivity to characterize solute spreading in environments with low-permeability lenses. Water Resources Research, 2002, 38(8): 7–14.

[15] AMAEFULE J O, ALTUNBAY M, TIAB D, et al. Enhanced reservoir description: Using core and log data to identify hydraulic (flow) units and predict permeability in uncored intervals/wells. SPE 26436, 1993.

[16] AL-DHAFEERI A M, NASR-EL-DIN H A. Characteristics of high-permeability zones using core analysis and production logging data. Journal of Petroleum Science & Engineering, 2007, 55(1/2): 18–36.

[17] GUO G, DIAZ M A, PAZ F J, et al. Rock typing as an effective tool for permeability and water-saturation modeling: A case study in a clastic reservoir in the Oriente basin. SPE Reservoir Evaluation & Engineering, 2007, 10(6): 730–739.

[18] RUSHING J A, NEWSHAM K E, BLASINGAME T A. Rock typing: Keys to understanding productivity in tight gas sands. SPE 114164 , 2008.

[19] ABEDINI A. Statistical evaluation of reservoir rock type in a carbonate reservoir. SPE 152359, 2011.

[20] TARIQ M, BIZARRO P, SOUSA A, et al. Reservoir characterization and modeling of a carbonate reservoir: Case study. SPE 161039, 2012.

[21] GHADAMI N, REZA RASAEI M, HEJRI S, et al. Consistent porosity-permeability modeling, reservoir rock typing and hydraulic flow unitization in a giant carbonate reservoir. Journal of Petroleum Science & Engineering, 2015, 131: 58–69.

[22] KONG Xiangyan. Advanced fluid mechanics in porous media. Hefei: China University of Science and Technology Press, 2010: 151–153.

[23] ZHU Huayin, MA Lining, CHEN Jianjun, et al. Research on characteristics of reservoir bed in Quaternary of Sebei-1 gas field. Natural Gas Industry, 2006, 26(4): 29–31.

[24] LI Xizhe, GUO Zhenhua, HU Yong, et al. Efficient development strategies for large ultra-deep structural gas fields in China. Petroleum Exploration and Development, 2018, 45(1): 111–118.

[25] WU Yongping, ZHU Zhongqian, XIAO Xiangjiao, et al. Fracture feature of Tertiary reservoir and distribution evaluation in Dina 2 gas field. Natural Gas Geoscience, 2011, 22(6): 989–995.

[26] LUO Ruilan, ZHANG Yongzhong, LIU Min, et al. Analysis of water invasion performance of ultra-deep and naturally fractured tight sand gas reservoirs. Journal of Zhejiang University of Science and Technology, 2017, 29(5): 321–327.

[27] HU Yong, LI Xizhe, WAN Yujin, et al. The experimental study of water inversion mechanism in fracture and the influence on the development of gas reservoir. Natural Gas Geoscience, 2016, 27(5): 910–917.

[28] LI Xizhe, GUO Zhenhua, WAN Yujin, et al. Geological characteristics and development strategies for Cambrian Longwangmiao Formation gas reservoir in Anyue gas field, Sichuan Basin, SW China. Petroleum Exploration and Development, 2017, 44(3): 398–406.

[29] LI Xizhe, LIU Xiaohua, SU Yunhe, et al. Correlation between per-well average dynamic reserves and initial absolute open flow potential (AOFP) for large gas fields in China and its application. Petroleum Exploration and Development, 2018, 45(6): 1020–1025.